The effects of high pressure and high temperature in semidilute aqueous cellulose nanocrystal suspensions

Saha, Sudeshna; Hemraz, Usha D.; Boluk, Yaman

Publisher's version / Version de l'éditeur:
https://doi.org/10.1021/acs.biomac.9b01130
Biomacromolecules, 21, 2, pp. 1031-1035, 2019-12-04

Biomacromolecules

Note

Cite This: Biomacromolecules 2020, 21, 1031−1035

pubs.acs.org/Biomac

The Effects of High Pressure and High Temperature in Semidilute Aqueous Cellulose Nanocrystal Suspensions

Sudeshna Saha,[†] Usha D. Hemraz,[‡] and Yaman Boluk*

Department of Civil and Environmental Engineering, University of Alberta, Edmonton, Alberta T6G 2R3, Canada

Supporting Information

ABSTRACT: A semidilute cellulose nanocrystal suspension was tested for pressure, volume, temperature dependencies of its viscosity and density. The compression of a 2.0 wt % cellulose nanocrystal suspension under 5.0 MPa at room temperature resulted in morphological changes from istotropic to nematic form. However, at high temperature, high-pressure treatment caused desulfation and gelation. Those results have significant applications, not only as additives in drilling and fracturing fluids but also for the preparation of hydrogels.

INTRODUCTION

Rod-shaped cellulose nanocrystals (CNC) are usually produced by concentrated sulfuric acid hydrolysis of a cellulosic biomass, and colloidally stable suspensions are formed in water due to the creation of negatively charged sulfate half ester groups on surfaces.[1] Applications of CNC particles in oilfields, such as rheology modifiers in drilling and fracking fluids at downholes with high pressures and temperatures, compelled us to undertake this study. Pressure−volume−temperature (PVT) effects on viscosity and density of CNC suspensions must be understood to develop density and hydraulics programs. In 2013, while we were working on experiments to investigate the equation of the state of CNC suspensions and the PVT diagrams under reservoir conditions, our findings from experiments on CNC particles under high pressure and temperature brought us new insights into the physical and chemical stability of CNC suspensions. Because of the confidentiality of the project, the results were not published earlier. In the meantime, Lewis et al. reported independently on gelation of aqueous CNC suspensions while conducting preliminary experiments on carbonization of CNCs under hydrothermal conditions.[2] Although their conclusion on the gel forming of CNC suspensions is similar, our experimental setup allowed to acquire data on specific volume changes vs pressure and temperature changes. Because of the importance of hydrogels, from biomedical applications to rheology modifiers, we were obliged to publish our results. Hence, we have described the physical and chemical alterations in a 2.0 wt % cellulose nanocrystal suspension under high pressure and temperature while still in its liquid state.

EXPERIMENTAL SECTION

Materials. Hardwood extracted cellulose nanocrystals obtained from Innotech Alberta (Edmonton, Alberta) pilot plant was used in this study. Cellulose nanocrystals are produced by milling the Northern Bleached hardwood Kraft pulp cellulose followed by concentrated sulfuric acid hydrolysis to remove the amorphous region and release cellulose nanocrystal whiskers.[3] CNC samples were fully neutralized Na version.

The colloidal CNC suspensions 2.0% and 0.1 wt % were prepared by dispersing the material in deionized water followed by sonication (Branson ultrasonic cleaner model 1510, frequency 40 kHz) for 3 min. Suspensions (0.1 wt %) were prepared in deionized water and filtered through a 0.45 μm filter membrane. The pH of the suspensions was 6.8 and no further pH adjustment was done.

The resulting 2.0 wt % suspension was used in high pressure−high temperature 0.1 wt % suspension was used for scanning electron microscopy, dynamic light scattering, and zeta potential measurements.

High Pressure−High Temperature (PVT) Treatment and Test. Samples were kept under high pressure and high temperature in a Schlumberger-DBR phase behavior system (Oilphase-DBR-Schlumberger). The heart of the system was a high-pressure PVT cell consisting of a glass cylinder (total sample volume 112 cm^3), secured between two full-length sight glass windows, inside a stainless steel frame. This design allowed for unimpaired visibility of the entire contents of the cell. Pressure was regulated through an automated, high-pressure, positive displacement pump (Oilphase-DBR-Schlumberger). The hydraulic fluid inside the pump was connected to a floating isolation piston located inside the PVT cell. The piston isolated the hydraulic fluid from the process side of the PVT cell. Controlled displacement of the isolation piston allowed for volume changes in the process chamber, thus providing an effective way to control pressure. The PVT cell was mounted inside a temperature-controlled air bath by means of a bracket, attached to a horizontal shaft. An electric motor powered the shaft, which oscillated through 60 degrees about its center of gravity at 40 cycles per minute. Temperature and pressure inside the PVT cell were monitored with a platinum RTD probe and a pressure transducer (both supplied with the phase behavior system).

Dynamic Light Scattering and Zeta Potential Measurements. The effective particle size and zeta potential of CNC particles before and after the high P−high T tests were determined by measuring electrophoretic mobilities of CNC particles using Nano ZS from Malvern (Worcestershire United Kingdom). Dynamic light scattering (DLS) measurements were used to measure translational diffusion constant of CNCs ad effective sizes of CNCs. Zeta potentials of CNCs were analyzed based on electrophoretic light scatting. The 4 mW He_Ne laser source wavelength for all the experimental analysis

Received: August 15, 2019
Revised: November 3, 2019
Published: December 4, 2019

DOI: 10.1021/acs.biomac.9b01130
Biomacromolecules 2020, 21, 1031−1035

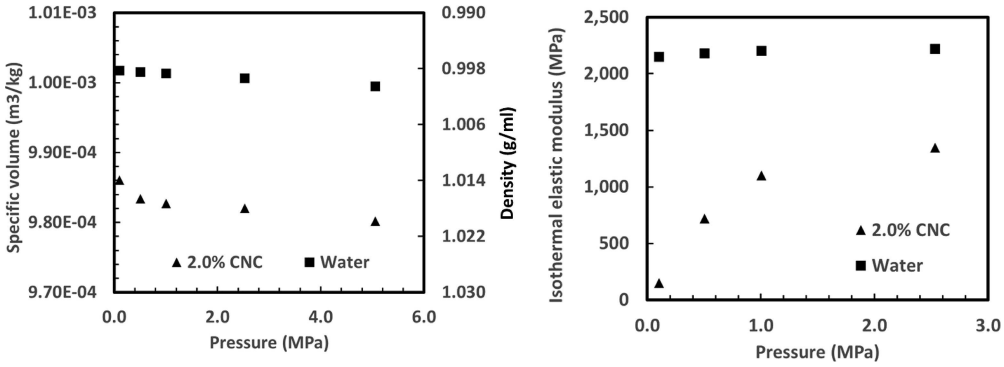

Figure 1. Specific volume (a) and calculated isothermal modulus K_T (b) of 2.0 wt % CNC suspensions and water at 20 °C.

was 633 nm. All the DLS and zeta potential experiments were carried out at room temperature (20 °C). The CNC concentration was 0.1% for all the tests. For repeatability, three measurements of each sample were taken. The hydrodynamic radius of CNC particles was measured as 70 ± 5 nm before the treatment under high pressure−high temperature experiments. The pH of the untreated 2.0 wt % CNC suspension was 6.8 and no further pH adjustment was done. There was no salt addition, and the conductivity of the untreated sample was less than <100 μS/cm.

Rheological Measurements. Steady state shear viscosity vs shear-rate measurements of CNC suspensions were carried out on a TA Instruments AR-G2 Rheometer (New Castle, DE) equipped with a 2° aluminum cone and plate geometry of 60 mm in diameter. The torque resolution was 0.1 μN.

TA Instruments AR-G2 rheometer equipped with a 2° aluminum cone and plate geometry of 60 mm in diameter was also used to measure linear viscoelastic properties of CNC before and after high P−high T test. The linear strain range was determined by carrying out strain displacement sweep at 1 rad/s. The oscillation mode tests were done at 1% strain which was within the linear range by sweeping the frequency between 0.1 and 100 rad/s. All of the measurements were done at 20 °C.

Scanning Transmission Electron Microscopy (STEM). The morphologies of the samples were investigated by high-resolution SEM using a Hitachi model S-5500 and SEM using a Hitachi model S-4800 apparatus equipped with a field emission source and operating at an accelerating voltage of 5 kV or 30 kV in transmission mode. A drop of the filtered colloidal suspension was deposited on a carbon-coated TEM grid for 3 min, and the excess suspension was wicked off using filter paper. The TEM grid was allowed to dry at room temperature for 3 min. The sample was then stained by depositing a drop of uranyl acetate solution (2.0 wt % in water) on the grid for 5 min. The excess solution was blotted using filter paper, and the grid was dried at rt for at least 24 h prior to imaging. The average width of CNC particles was measured as 8 ± 0.8 nm from STEM micrographs before the treatment under high pressure−high temperature experiments.

RESULTS AND DISCUSSION

Compression under Room Temperature. Specific volume vs pressure results of 2.0 wt % CNC suspension and water at 20 °C are shown in Figure 1. The addition of CNC into water caused a decrease in specific volume (with an increase in density). The CNC suspension has a steeper specific volume function of pressure than water. The decrease of specific volume of the CNC was more drastic between atmospheric pressures and 400 kPa. 2.0 wt % CNC was more compressible than water and its compressibility increases more at high pressures.

The data in Figure 1 was used to calculate the isothermal elastic modulus of the CNC suspension and water by numerical differentiation according to[4]

$$K_T = -V\left(\frac{\partial P}{\partial V}\right)_T \quad (1)$$

where K_T, P, V, and T are isothermal elastic modulus, pressure, specific volume, and temperature. Figure 1b presents the calculated isothermal elastic modulus of 2.0 wt % CNC suspension and water at 20 °C. The calculated K_T values of water increased from 2.1 to 2.2 GPa within the range of 100−3000 kPa, and are comparable with previously reported findings.[5−7] The addition of 2.0 wt % cellulose nanocrystals lowered the isothermal elastic modulus of water. This result showed that the macroscopic compressibility (the inverse of the isothermal elastic modulus) of a 2.0 wt % CNC suspension is increased under pressure because of the transition from isotropic to nematic structure under pressure. Particle−particle interactions among rod-shaped CNC particles are higher in the case of parallel orientation than cross orientation. Random isotropic structure is favored due to the lower energy of interactions among cross oriented particles.[8] However, increasing the pressure on the sample volume overcomes the higher interaction energy among parallel-oriented CNC particles, and results in a nematic structure. The increase of illumination with applied pressure under cross polarizer observed during the high pressure test confirmed the ordered structure of cellulose nanocrystals (Figure 2a). The compressibility of CNC suspension under pressure is schematically illustrated in Figure 2b with isotropic to nematic transition. Stability of isotropic nematic and smectic phases of rod-like molecules and colloidal particles are investigated by computer simulations. First Frenkel reported isothermal−isobaric Monte Carlo and molecular dynamics simulations for a system of 576 rod-like molecules with aspect ratio (L/D) of 5, which formed isotropic, nematic, smectic, and solid phases.[9] According to this simulation, the nematic phases were obtained by compressing the isotropic states, but the compression procedure was abandoned at the nematic−smectic transition; instead the smaller system was slowly melted from the solid into the smectic phase. Later, Veerman and Frenkel reported a tentative phase diagram for the hard spherocylinders with arbitrary aspect ratio, nevertheless leaving open the question of whether the nematic or the smectic-A is the first liquid crystalline phase to appear for spherocylindrical rods with intermediate aspect ratios.[10] Our experimental results also showed the formation of ordered structure under the

DOI: 10.1021/acs.biomac.9b01130
Biomacromolecules 2020, 21, 1031−1035

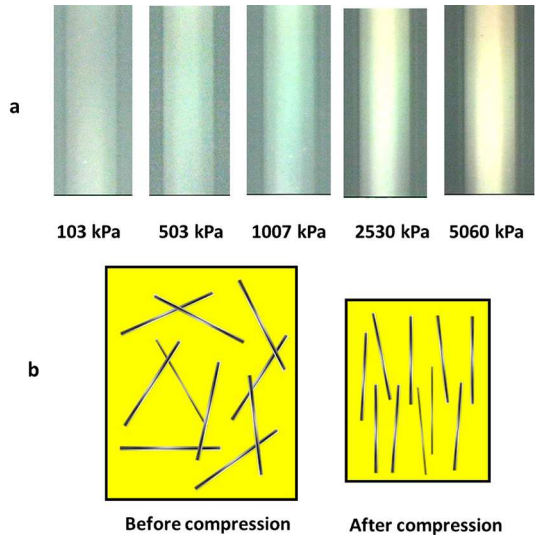

Figure 2. Pictures of the test cell while pressure was increasing from 103 to 5060 kPa at T = 20 °C (a), schematic representation of isotropic to nematic transition under compression (b).

compression of isotropic CNCs which have the aspect ratio (L/D) of 8.

Thermal Effect at 5.0 MPa. The specific volume change with temperature at 5.0 MPa pressure for a 2.0 wt % CNC dispersion was compared with that of water (Figure 3). The

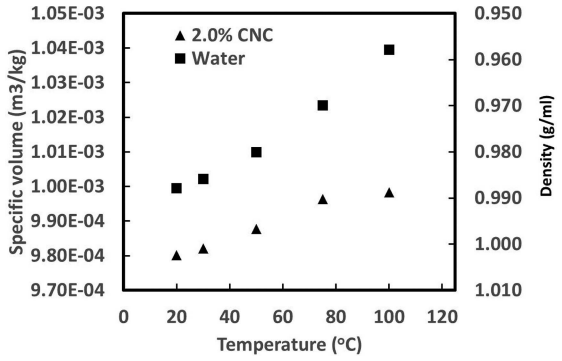

Figure 3. Specific volume of 2.0 wt % CNC suspension and water at 5.0 MPa.

specific volume of 2.0 wt % CNC was lower than that of water at all temperatures. This was due to the higher density of the CNC dispersion than that of water. The thermal expansion of both water and 2.0 wt % CNC increased with an increase in temperature. Nevertheless, the steady increase of a specific volume of 2.0 wt % CNC halted around 80 °C. The whole experiment at 5.0 MPa lasted 24 h, but only 3 h of pressurization occurred during temperatures between 80 and 100 °C.

Three hours of treatment at high pressure (5.0 MPa) and high temperature (80−100 °C) converted 2.0 wt % CNC suspension to a semisolid gel (Figure S1). Structural information on 2.0 wt % CNC suspension before and after the treatment was obtained by conducting frequency sweeps at 1.0% strain (within the linear deformation range) as shown in Figure 4. In the case of untreated 2.0 wt % CNC suspension, a viscoelastic fluid response was observed with a crossover point of G' and G'' at around 1 rad/s. At the low frequency range

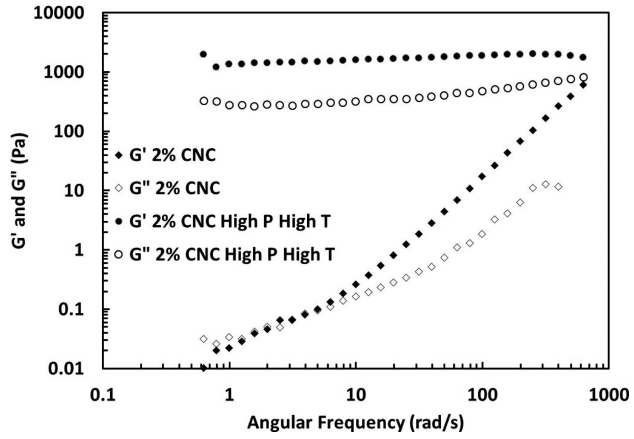

Figure 4. Storage (G') and loss modulus (G'') of 2.0 wt % CNC suspension before and after high-pressure and high-temperature treatment.

(<1.0 rad/s), the viscous component G'' is higher than the elastic G' component. The elastic component G' increased faster than the viscous component G'' with increase in frequency and $G' > G''$ was above the crossover point. However, a semisolid gel like response was observed after high P and high T treatment of 2.0 wt % CNC suspension. G' was higher than G'' over the entire frequency spectrum and independent of oscillation frequency. This is due to the aggregation of CNC particles after the treatment. Similar rheological behavior is observed with a 4.0 wt % CNC suspension after hydrothermal treatment in an autoclave after 20 h of treatment at temperatures above 80 °C.[2]

Figure 5 shows the steady state shear viscosities of high pressure - high temperature (high P−high T) treated 2.0 wt %

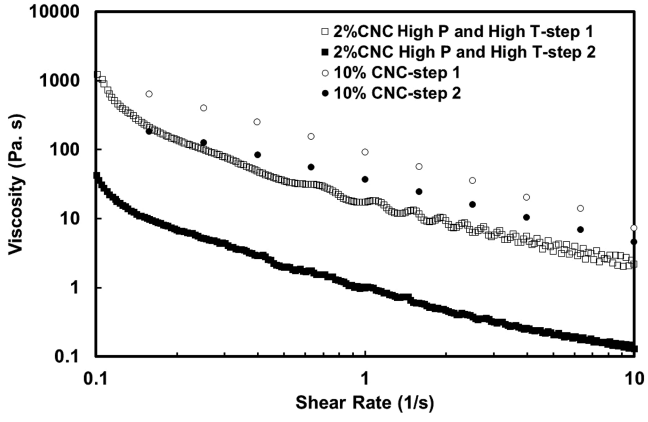

Figure 5. Steady shear viscosities as a function of shear rate for high P and high T treated 2.0 wt % and untreated 10 wt % CNCs suspensions. Step 1 and Step 2 plots show samples before and after shearing at 100 s^{-1} for 5 min, respectively.

CNCs gel along with untreated 10.0 wt % CNCs suspension. Step 1 plots are the viscosity vs shear rate plots of those samples without carrying preshearing procedure before the viscosity measurements. As reported previously, the shear viscosity of untreated 2.0 wt % CNCs suspension is comparatively very low (<0.5 Pa.s at 0.1 s^{-1}) and almost shear rate independent (Newtonian).[11,12] Therefore, instead of untreated 2.0 wt % CNC suspension, untreated 10.0 wt % CNCs suspension was selected to show the magnitude of

DOI: 10.1021/acs.biomac.9b01130
Biomacromolecules 2020, 21, 1031−1035

Table 1. Elemental Analysis of CNC Samples before and after the High P−High T Test

sample 2.0 wt % CNC	nitrogen	carbon (wt %)	hydrogen (wt %)	oxygen (wt %)	sulfur (wt %)
before high P−high T	0	40.34 ± 0.11	5.92 ± 0.07	53.06 ± 0.15	0.55 ± 0.11
after high P−high T	0	40.95 ± 0.09	6.3 ± 0.03	52.77 ± 0.04	0

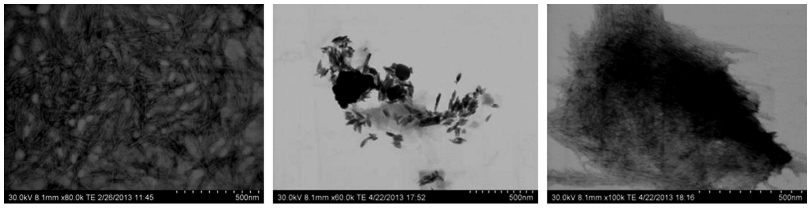

a b c

Figure 6. STEM image of CNC: before (a) and after high P−high T test (b,c).

thickening effect due to the treatment. Pressure and temperature treatment of 2.0 wt % CNCs resulted in very high viscosities at all shear rates. It is worth to note that the viscosity of 2.0 wt % treated sample was trending to exceed the viscosity of 10% untreated sample at shear rates less than 0.1 s^{-1}. On the other hand, the viscosity of the treated 2.0 wt % CNCs sample was somewhat lower than the untreated 10.0 wt % CNCs at shear rates higher 0.1 s^{-1} by exhibiting more stronger non-Newtonian the shear thinning behavior. Treated 2.0 wt % CNC suspension, which was in fact a semidilute suspension,[13] resulted in higher viscosities at low-shear rates and lower viscosities at high-shear rates than the untreated but concentrated 10 wt % CNC suspension. The treated 2.0 wt % CNC solid-like gel was more shear thinning with the steeper viscosity vs shear rate behavior than the untreated 10.0 wt %. The steeper non-Newtonian behavior of treated 2.0 wt % CNC was due to the presence of fewer but flocculated CNC particles. Increasing the shear rate disrupts them easier than crowded particles in the case of 10 wt % CNC. Shear dependent non-Newtonian viscosity is one of the most important desired property of any thickening agent offer in functional fluid formulations whether they are coatings, drilling fluids, personal care products or sprayable liquids. Always low viscosities at higher shear rates permits easy pumping, spraying or any kind of fluid transport and application. In the meantime, high viscosities at low shear rates are needed to stick the fluid on sloped surfaces or suspend colloidal particles in them.

Step 2 plots in Figure 5 shows viscosity vs shear rate measurements just after 5 min of preshearing of samples at 100 s^{-1} for 5 min. In this case the viscosity of treated 2.0 wt % CNC sample decreased 2 orders of magnitude, nevertheless the sample still showed a shear thinning behavior. Step 2 preshearing procedure reduced the viscosity of untreated 10.0 wt % CNCs suspension 1 order of magnitude at low shear rates but at high shear rates (>10 s^{-1}) the viscosities of Step 1 and Step 2 measurements were converging. Nevertheless, those viscosity drops of both of those samples after preshearing were not permanent and viscosities recovered to the original states in 10 min, which means they were thixotropic.

The elemental analysis results showed the desulfation of CNC particles after the high pressure-high temperature treatment (Table 1). Dorris and Gray[14] observed desulfation of CNC (H version) particles by autocatalytic hydrolysis during a slow evaporation process in the presence of glycerol leading to thixotropic gel. In another study, Lewis et al. also observed desulfation after the hydrothermal treatment of a 4.0 wt % CNC suspension.[2] The surface sulfate ester groups play a very important role in stabilizing the CNC dispersion in water by electrostatic repulsion. The decrease in sulfate ester groups decreases the electrostatic repulsion among CNC particles and leading to aggregation particles. In this present study, a complete truncation of the sulfate ester group from the CNC particles leads to a stable aggregated phase after the high pressure-high temperature treatment. In an autoclave gelation of CNCs, Lewis et al.[2] reported that hydrothermal treatment selectively catalyzes the hydrolysis of negatively charged sulfate half ester groups on surfaces rather than formation of amorphous cellulose network and degradation of CNC particles. According to FTIR analysis, there was no extra peak or lesser peak was observed for CNCs as compared to that of the CNCs after high P−high T (Figure S2).

The colloidal stability of the aqueous dispersion of CNC before and after the high pressure-high temperature treatment was investigated by zeta potential measurements without adjusting the pH. The CNC particles without treatment showed high negative zeta potential value (−56.8 ± 2.1 mV). As expected this was due to the presence of negatively charged sulfate half ester groups on the surfaces of CNCs which were formed during the sulfuric acid hydrolysis. However, the desulfation process eliminated the negative surface charges.

The suspension was expected to become more acidic due to with elimination of sulfate half ester groups acid and formation of free sulfuric acid. Therefore, the zeta potential increased significantly after the high pressure-high temperature treatment to −11.46 ± 0.9 mV. The zeta potential values for CNC before and after the treatment suggest a high stability of CNCs before the treatment and a coagulation potential of CNC dispersion after the desulfation.[8] The stability of CNC suspensions is controlled by the sum of the attractive van der Waals forces and the electrical double layer repulsion between the particles.[8] Hence, CNC particles with less than zeta potential of −15 mV start to flocculate instantaneously.[15]

The increase in zeta potential value suggest the instability of the CNCs dispersion after the high P−high T test, and the flocculation of dispersion. The dynamic light scattering results show average particle size of CNC before HPHT test is around 138 nm whereas average particle size of CNC after HPHT test is 2701 nm. As expected also from zeta potential results, this was due to aggregation of CNC particles during HPHT test.

The STEM analysis of the CNC nanoparticles before and after the high P−high T test (Figure 6) revealed the stark difference between those two samples. As expected, the CNC

DOI: 10.1021/acs.biomac.9b01130
Biomacromolecules 2020, 21, 1031−1035

nanoparticles before the treatment were well-dispersed. After the test, the morphologies of CNC nanoparticles showed two different kinds of structure. In one of the images after the high P−high T test (Figure 6b), the average length of the cellulose nanocrystals was observed to be around 75−100 nm, and the orientations were mostly parallel. It shows the existence of nematic structure due to compression of the suspension. Nano particles of CNC were aggregated in a parallel orientation after the high P−high T test. In another image (Figure 6c), it was found that the CNC particles aggregated to form a mesh-like structure in which it was very difficult to identify a single CNC particle. Those two STEM pictures shows nonhomogenous nature of the hydrothermally treated CNC suspension.

CONCLUSIONS

The growing importance of applications of CNC particles in oilfield applications such as additives in drilling and fracking fluids at high pressures and temperatures compelled us to undertake this study. While leading experiments to investigate the equation of the state of CNC suspensions under reservoir conditions, the information gathered on CNC particles under high pressures and temperatures opened new doors of applications in production of hydrogels. At room temperature, the compression of cellulose nanocrystal suspension resulted in orientation and an istotropic to nematic transition. However, 5 MPa pressure at 80 °C caused the aggregation and gelation of CNC particles. The rheological results showed that the 2.0 wt % CNC suspension after the high P−high T treatment behaved similarly to that of untreated 10.0 wt % CNC dispersion. Further investigation suggested detachment of surface sulfate ester groups from CNC particles, resulting in an aggregated state observed after the high P−high T treatment. Downhole temperature−pressure conditions did not generate any negative effect on CNCs. On the contrary those high temperature-high pressure conditions enhanced the thickening efficiency CNCs by also chemically modifying surfaces of CNCs.

Desulfation and elimination of half ester sulfate groups under high pressure and high temperature will be an interest to produce CNCs as rheology modifiers not only for drilling fluids but also in other functional fluid formulations such as paints coatings, personal care products or sprayable liquids. In addition, high pressure and high temperature treatment can also used for the generation of hydrophobic CNCs which would be an interest to disperse CNCs in nonpolar media.

ASSOCIATED CONTENT

Supporting Information

The Supporting Information is available free of charge at https://pubs.acs.org/doi/10.1021/acs.biomac.9b01130.

Photographs of CNC suspension before and after the HP-HT treatment (Figure S1), FTIR analysis of CNC particles before (a) and after high P−high T treatment (b) (Figure S2), X-ray photoelectron spectroscopy (XPS) results before and after high P−high T test (Figure S3 and S4), and Deconvoluted C 1s peak and concentration of different bands (Table S1) (PDF)

AUTHOR INFORMATION

Corresponding Author

*E-mail: yaman.boluk@ualberta.ca.

ORCID

Yaman Boluk: 0000-0003-1837-6527

Present Addresses

†S.S.: Department of Chemical Engineering, Jadavpur University, Kolkata 700 032, India

‡U.D.H.: National Research Council, Montreal, Quebec H4P 2R2, Canada

Notes

The authors declare no competing financial interest.

ACKNOWLEDGMENTS

This research was supported by Alberta Innovates. The authors thank Alberta Innovates and its industrial partner, Innotech Alberta.

REFERENCES

(1) Klemm, D.; Kramer, F.; Moritz, S.; Lindström, T.; Ankerfors, M.; Gray, D.; Dorris, A. Nanocelluloses: a new family of nature-based materials. *Angew. Chem., Int. Ed.* **2011**, *50* (24), 5438−5466.

(2) Lewis, L.; Derakhshandeh, M.; Hatzikiriakos, S. G.; Hamad, W. Y.; MacLachlan, M. J. Hydrothermal gelation of aqueous cellulose nanocrystal suspensions. *Biomacromolecules* **2016**, *17* (8), 2747−2754.

(3) Esparza, Y.; Ngo, T.; Fraschini, C.; Boluk, Y. Aggregate Morphology and Aqueous Dispersibility of Spray-Dried Powders of Cellulose Nanocrystals. *Ind. Eng. Chem. Res.* **2019**, *58*, 19926.

(4) Korolovych, V.; Bulavin, L.; Prylutskyy, Y. I.; Khrapatiy, S.; Tsierkezos, N.; Ritter, U. Influence of single-walled carbon nanotubes on thermal expansion of water. *Int. J. Thermophys.* **2014**, *35* (1), 19−31.

(5) Hayward, A. How to measure the isothermal compressibility of liquids accurately. *J. Phys. D: Appl. Phys.* **1971**, *4* (7), 938.

(6) Korolovych, V.; Nedyak, S.; Moroz, K.; Prylutskyy, Y. I.; Scharff, P.; Ritter, U. Compressibility of water containing single-walled carbon nanotubes. *Fullerenes, Nanotubes, Carbon Nanostruct.* **2013**, *21* (1), 24−30.

(7) Heggen, R. J. Thermal dependent physical properties of water. *Journal of Hydraulic Engineering* **1983**, *109* (2), 298−302.

(8) Oguzlu, H.; Danumah, C.; Boluk, Y. Colloidal behavior of aqueous cellulose nanocrystal suspensions. *Curr. Opin. Colloid Interface Sci.* **2017**, *29*, 46−56.

(9) Frenkel, D. Structure of hard-core models for liquid crystals. *J. Phys. Chem.* **1988**, *92* (11), 3280−3284.

(10) Veerman, J.; Frenkel, D. Phase diagram of a system of hard spherocylinders by computer simulation. *Phys. Rev. A: At., Mol., Opt. Phys.* **1990**, *41* (6), 3237.

(11) Lu, A.; Hemraz, U.; Khalili, Z.; Boluk, Y. Unique viscoelastic behaviors of colloidal nanocrystalline cellulose aqueous suspensions. *Cellulose* **2014**, *21* (3), 1239−1250.

(12) Shafiei-Sabet, S.; Hamad, W. Y.; Hatzikiriakos, S. G. Rheology of nanocrystalline cellulose aqueous suspensions. *Langmuir* **2012**, *28* (49), 17124−17133.

(13) Oguzlu, H.; Boluk, Y. Interactions between cellulose nanocrystals and anionic and neutral polymers in aqueous solutions. *Cellulose* **2017**, *24* (1), 131−146.

(14) Dorris, A.; Gray, D. G. Gelation of cellulose nanocrystal suspensions in glycerol. *Cellulose* **2012**, *19* (3), 687−694.

(15) Hemraz, U. D.; Lu, A.; Sunasee, R.; Boluk, Y. Structure of poly (N-isopropylacrylamide) brushes and steric stability of their grafted cellulose nanocrystal dispersions. *J. Colloid Interface Sci.* **2014**, *430*, 157−165.

DOI: 10.1021/acs.biomac.9b01130
Biomacromolecules 2020, 21, 1031−1035